POLITECNICO DI TORINO

Master of science program in Energy and Nuclear Engineering

Course of Wind and Ocean Energy Plants - 01TVKND

PW.2 – PRE-DESIGN OF A WAVE ENERGY CONVERTER

Team n. 44

Qifan Zhu, s288338

Tianmeng Yan, s287593

Yuwei Shi, s288123

A.Y. 2023/24

Table of contents

List of figures

List of tables

1. Wave resource assessment

This project will try to analyze a point absorber for ocean energy located nearby the island of Pantelleria in Sicily (IT), hence, to assess the wave energy available in the area in four years of interest (1982 1986 1994 and 2012). Then, a wave farm will be analyzed in terms of productivity in both time and frequency domain and an economic analysis of such farm will be computed.
The first step is to analyze the wave energy available at this location.

1.1 Energy and occurrences scatters

To analyze the energy that can be extracted from this site we needed to evaluate both the energy for the waves and the occurrences for such waves (meaning how often a wave with such energy strike the site). This for the full period of examination. In order to show an idea of the occurrences, the wave scatters for the significant wave height H_s (defined as the mean of the highest third of the waves) and the wave energy period T_e are reported for the years 2012 and 1982. Those parameters are relevant as the power of the waves can be expressed as a function of $H_s^2 * T_e$

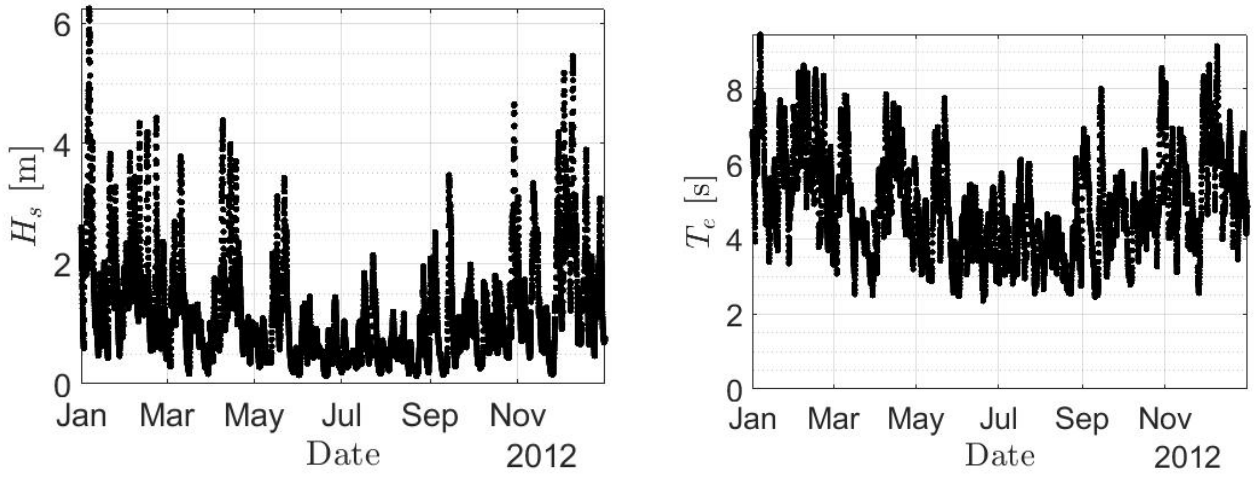

Figure 1: Hs and Te scatter 2012

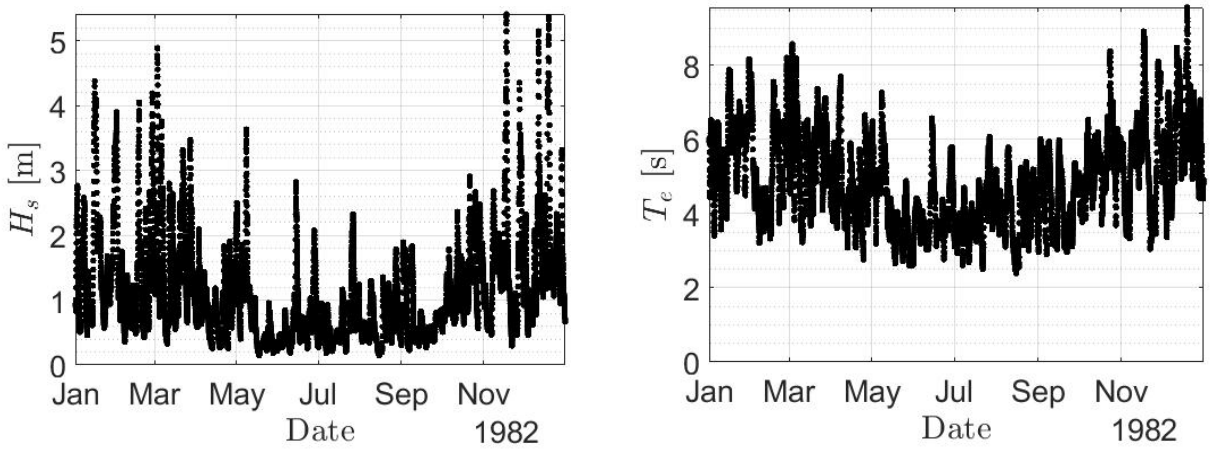

Figure 2:Hs and Te scatters 82

As it can be seen from the figures 1 and 2, the waves behavior during two years of sampling made 30 years apart from each other show somewhat a similar behavior, with reasonable differences on particular dates where probably there were stronger winds than the average. Both in terms of period and wave height, this site is expected to be more productive in the cooler months (from October/November to April/May).

1.2 Directional waves analysis

The next step is to analyze the wave direction, this analysis will provide information about the likeability of the way to travel towards a certain direction of the wave rose. Here as well, two significant scatters graph for years 2012 and 1982 will be provided, along with the wind rose for the overall period of study of the four aforementioned years.

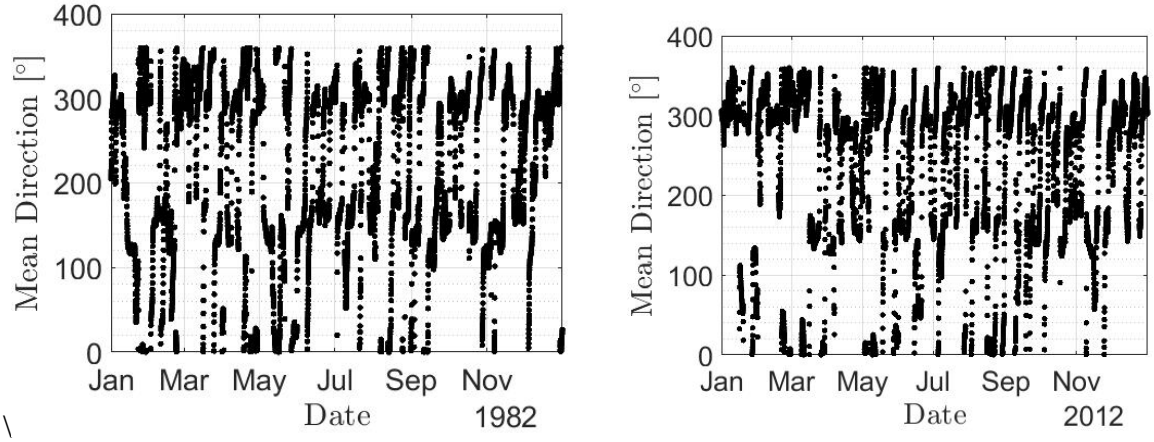

Figure 3: mean wave direction for years 1982 and 2012

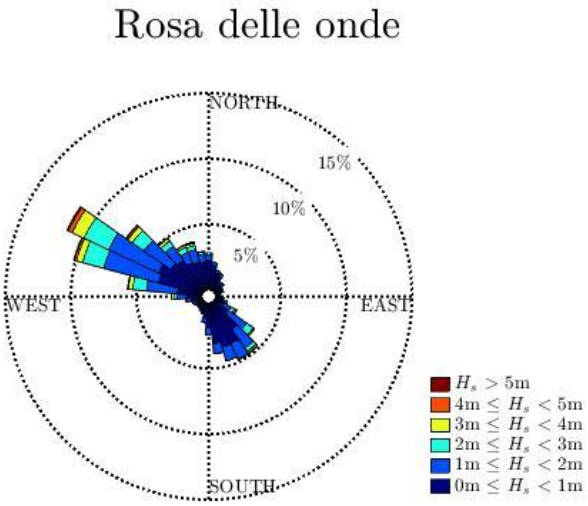

The scatters plots show us that, on average, the main wave direction is the one enclosed in the part of the plot above 270^o, this is in compliance with what the wave rose for the whole period tells. In fact, in the directions N-W and W-N-W we can observe both the highest wave occurrence and the most relevant weave height in the spectrum. In fact, in Pantelleria the currents flow mainly across a channel which is in compliance with this direction.

Figure 4. wind rose for the whole period

1.3 Cumulative analysis – occurrences and energy

In this section a cumulative analysis for the whole 4 years period will be performed. This analysis will allow to have a better understanding of how the various parameters and occurrences alike influence the energy production.

1.3.1 Te

The wave period in this site has a peak in the occurrences at about 4 seconds, but its energy density is highest at about 7, this essentially means that the cumulative energy contribution of a highest occurrence waves is less energetic than the lower occurrence waves that comes at a higher period.

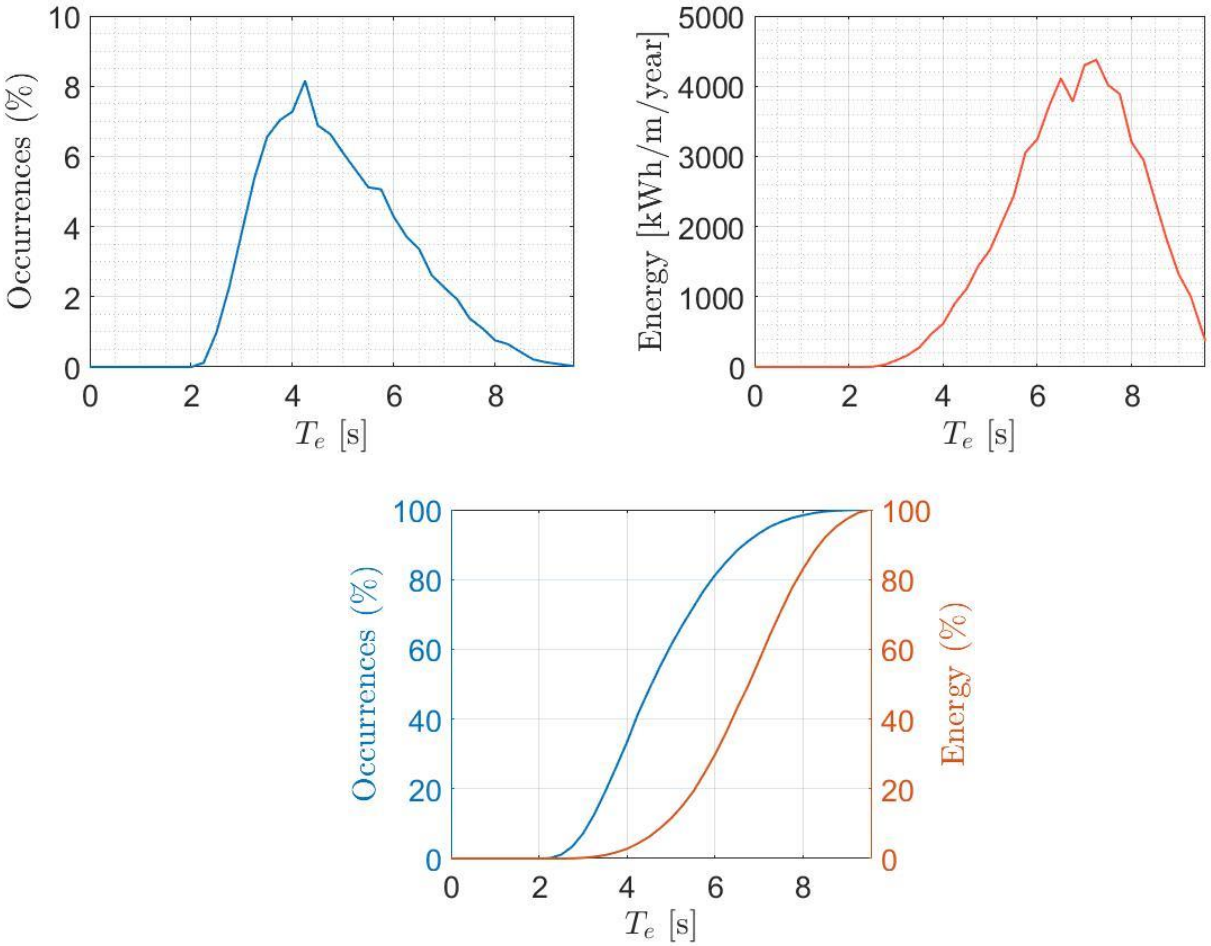

Figure 5: evaluations on Te

1.3.2 Hs

An analogous consideration can be made for Hs as the most energetic waves are about 1m high but the energy density is mostly distributed throughout about 2 m.

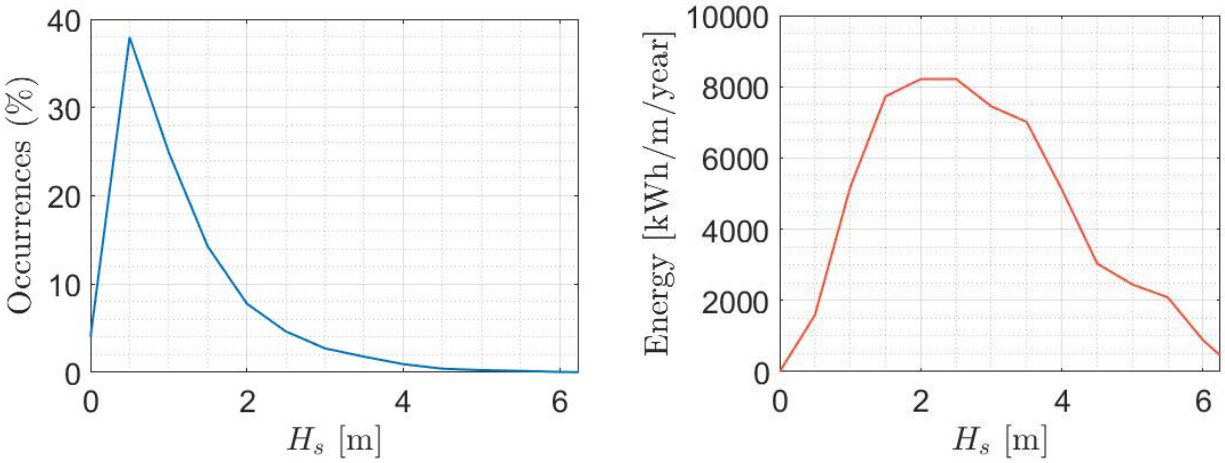

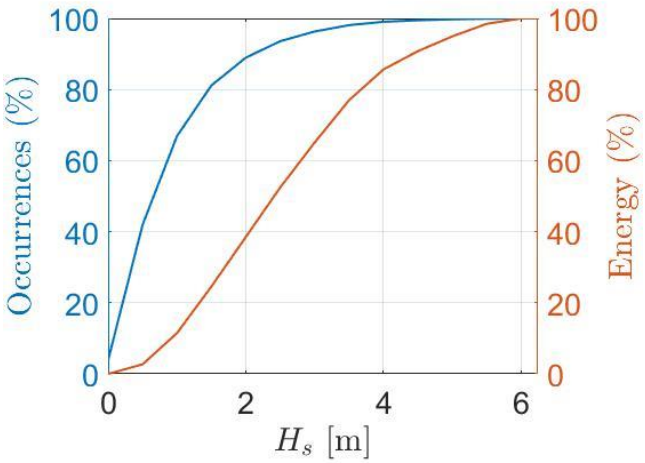

Figure 6: Evaluations on Hs

1.3.3 Matrixes

In figure XX the occurrences of a wave with the abscissa's wave period and the ordinate's wave height are shown. From this it is possible to see that the most probable waves have a $H_s$of less that 1 meter with a $T_e$that mostly spans from 3 to 5 seconds. The plot follows the characteristic trend for the wave occurrences of upward right slope (meaning that no waves will be had with a short-wave period and high characteristic height and vice-versa)

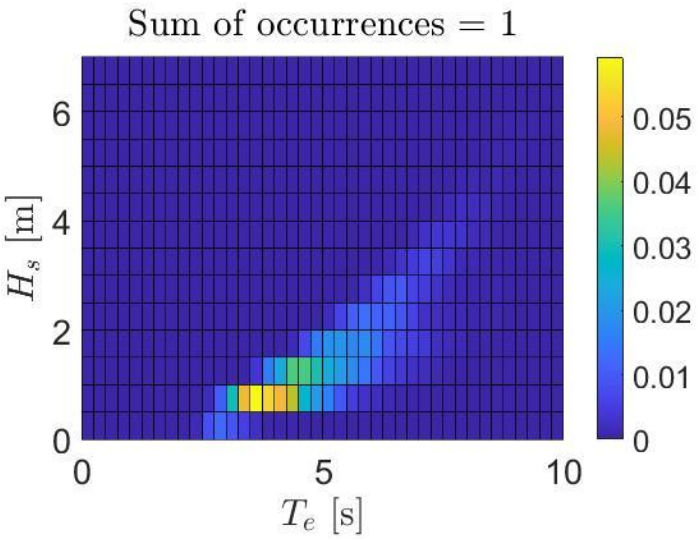

Figure 7: Cumulative analysis: occurrences plot

Figure 7 shows instead the mean energy per meter of absorber that can be extracted from the wave in a year. Basically, summarizing all the aforementioned considerations, we can see that there is a strong mismatch between the highest occurrence waves and the most energetic ones. In fact, the most energetic waves are more scattered towards a 5 to 10 second period and with a height of more than 2 m.

Also in this case, the plot follows the upward right sloped trend typical of the wave behavior.

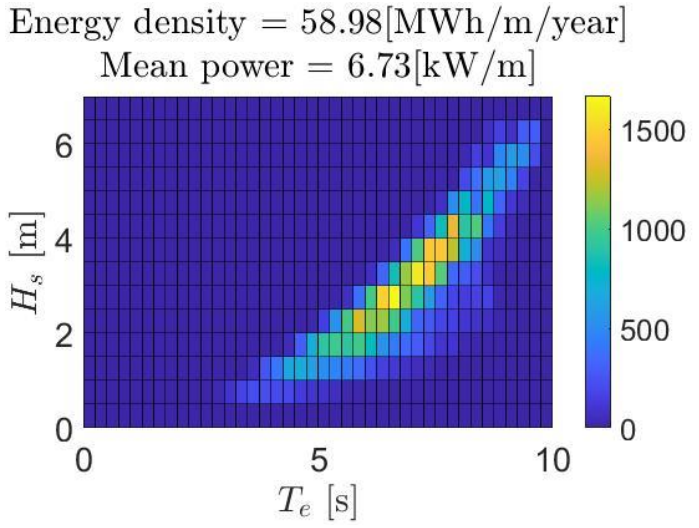

Figure 8: cumulative analysis: energy plot

1.4 Bathymetry analysis and site location

The final stem has been to study the bathymetry of the site and to locate the point absorber according to some constraints. The first constraint was about the influence of a shallower water (which would reduce significantly the performances of an absorber). In order to comply with such constraint and according to literature we need to lay our absorber at a height equal to

$$h > \frac{\lambda}{2}$$

where λ is the wavelength. In the Mediterranean sea, this condition is always respected for a seafloor depth of about 40 meters.

Then, there is the constraint of minimal distance from the coast which has to be at least 1 km. It is to be kept in mind that the further away the farm is from the coast, the more I will need to spend for cables and infrastructure to operate such farm.

In our case: we decided to place the point absorber at a distance of 1.0879 [km] from the coast as shown in the figure below.

The coordinates at which the distance was calculated are:

Point on the coast:

```
lon = 11.93
lat = 36.80
```

Point of the farm

```
lon = 11.93
lat = 36.79
```

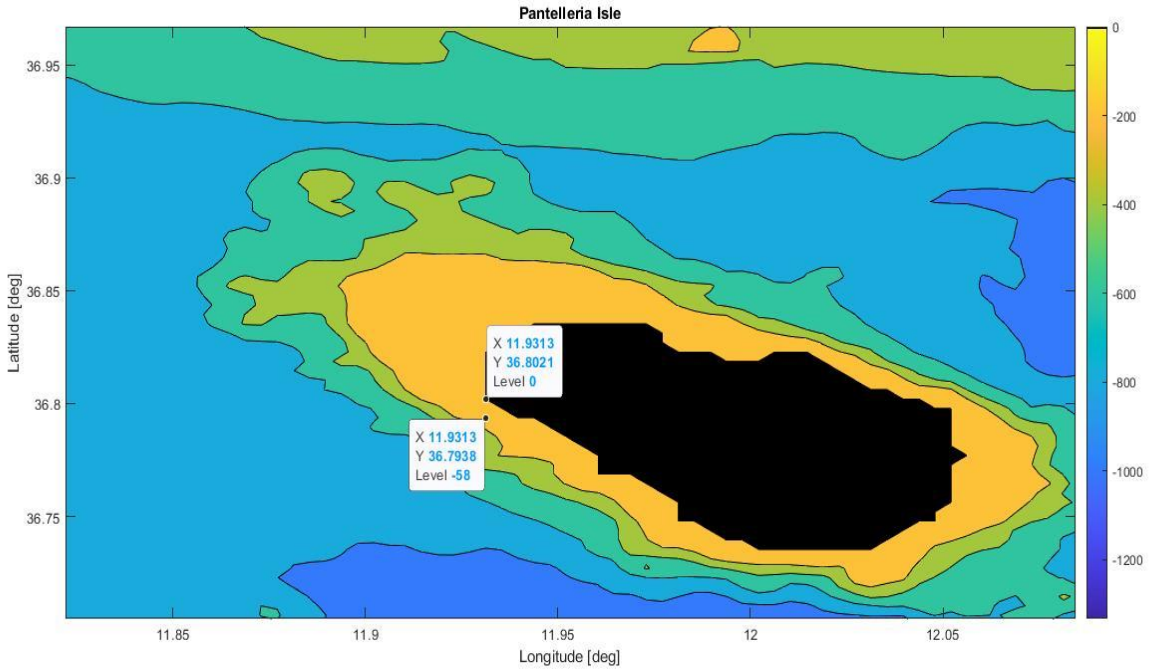

Figure 9: Site map

2. Frequency domain simulations

The hydrodynamic interaction between wave energy converters and ocean waves is a complex high-order nonlinear process.
There are different ways to compute hydrodynamic interactions. The most general follow the Navier-Stokes equations, which are the most accurate, because they take into account all interactions, but they are really slow to compute and not feasible for extensive studies. However, under particular conditions, there are fully linear models that are based on the assumption on incompressible flow, which is an acceptable approximation for liquids. The continuity equation becomes:

$$\nabla u = 0,$$

where u(x,y,z) denotes the fluid velocity vector. Moreover, another assumption is based on irrotationality of the fluid:

$$\nabla \times u = 0$$

Under these conditions, it is possible to express the velocity potential, according to:

$$u = \nabla \phi$$

By substituting the third equation on the first, in the fluid domain the velocity potential must satisfy the second order partial differential equation, called Laplace's equation:

$$\nabla^2 \phi = 0$$

In this way, it is possible to use this potential in order to define some characteristics of the device. This potential is computed by boundary element method (BEM) software. In the following study, Nemoh software was considered.
Frequency domain analysis is the first step in the validation of the merits of the design under operational sea conditions. The analysis provides a first step in the design process. The aim is to define the parameters of the wave energy converter (WEC), to define a mooring configuration and power take-off system, and to get a first impression how the devices will perform.
During the process, relevant results are Response Amplitude Operator (RAO), Froude-Krylov forces, diffraction forces, added mass, and radiation damping forces in the frequency domain. Hydrostatic results can also be extracted.
By analyzing an iterative approach to changing shape design, results provide greater power output. This will be a first step in the process to estimate a cost of energy for the device and the Cost over Productivity (CoP).

2.1 Simulation parameters definition

The considered WEC is like point absorber one. This device has considerably smaller dimensions than a wavelength and can produce power independently of the direction of wave propagation. This concept is inspired by a successful wave energy device, that is called Corpower, based in Sweden, and it is one of the most successful.
The software can be run for arbitrary geometry or, in this case study, for axial symmetric geometry, since it is the most forward and the simplest to analyze.
The device is characterized by a cylindrical shape, in which points among x-z plane are going to be the vertex points where geometry changes. Three points are needed:

- A point above the water, in which the z coordinate has a positive value.
- A point that constructs the cylindrical geometry, with negative z value.
- A point in which z coordinate has a negative value, so it is a point below seawater level.

The x coordinate represents the length of the radius: in fact, on the point above the water and on the point in sea level, it assumes a positive value, equal to the radius. On the point below, it is equal to zero, in order to consider a bottom disk and to close the geometry. The choice of cylinder is due to the fact that it is a simple geometry, in order to perform some parametric studies. Even if a point above the seawater level has been defined, the hydrodynamic analysis is performed up to z = 0, so, for whatever portion of the body is wet, when there are no coming waves.
One of the assumptions of the linear wave models is that wave amplitude is really small. So, the code assumes that the wet portion of the body is always the same.
A reference point is defined, centered into the origin of coordinate system (0,0,0), which is the seawater level. This is the point where the forces and coefficient are computed.
The way the software works is to define a mesh, a spatial discretization of the surface. Since an axial symmetric floater is considered, this mesh has different angles of discretization, equal to 35, around z axis. The considered number of panels that the mesh has considered is 800.
Frequencies where the characteristics of device are analyzed, by means of the wavelength, and considered. The diameter D of the device is the characteristic dimension, while the wavelength λ is in the range between 0.25 and 250 times the dimension: 80 equally spaced frequencies are studied. Deep water approximation is carried out, in order to explain the correlation between frequency and wavelength.
Wave direction is also defined, imposed equal to zero. This means that the waves are travelling along positive x direction. According to the direction, the behavior and hydrodynamic coefficients are in general different, but, in axial symmetric analysis, it does not really count.

As already said, the case study regards a cylindrical shape. The buoyancy force is totally equal to the displacement force of the point absorber. In the script, there are different properties for the materials, starting from the density, up to the thickness and costs. The thickness vector is function of the radius of cylinder. To find the best inertial properties of the WEC, buoyancy percentage is fixed, that can be

considered as percentage of water density. In this study case, it is equal to 0.66, which means that the 34% of its height will float above the seawater level.
Finally, starting with parametric run, parameters for the model are set, which are:

- Radius r, defined as a parametric vector of 8 elements.
- Fraction r/h, defined as a parametric vector of 9 elements.

The boundaries are:

$$\begin{cases} 1\,m < r < 10\,m \\ 1.5 < \dfrac{r}{h} < 3.5 \end{cases}$$

2.2 Parametric run

This part regards the launch of Nemoh software. Although the software solves for motions and forces in 6 degreed of freedom, initially, due to computational reasons, the analysis is carried out on the heave motion. Thus, only motion in the z-direction is analyzed. Since a parametric run was performed, all the outputs are in the matrix structure form, which are not totally reported, for simplicity. The outputs data of the simulation are:

- Added mass A.
- Radiation dumping B.
- Excitation force.
- Froude-Krilov and diffracted components of the excitation force.
- Responde Amplitude Operator (RAO).
- Hydrostatic data.

It is necessary to simplify and to linearize the forces involved. Thus, in accordance with linear wave theory, fluid motion and the motion of amplitude of the device are assumed sufficiently small for viscous effect to be neglected.
The equation of the motion results in the Cummins equation:

$$(m + A)\ddot{\xi} + B\dot{\xi} + K\xi = \sum_{i=1}^{N} f_{ext,i}$$

A represents the mass of water that moves with the body in the water, while B represents the damping that the body experiences in the water. These coefficients are respectively proportional to the acceleration and

to the velocity, which define, in the frequency domain, the radiation force. This one is defined as the force that it is needed to apply on a buoy, in order to perform harmonic motion.
The excitation force is defined as the force that a floater is feeling when it is kept fixed in a position and waves are incoming and hitting itself. This force is defined in two components:

$$F_e(\omega) = F_{FK}(\omega) + F_d(\omega)$$

where:

- $F_{FK}(\omega)$ is the part that analyzes how the forces of an undisturbed wave field would exert on a floater. This considers the no disturbance of the floater.
- $F_d(\omega)$ is the part that describes how the presence of the floater disturbs the field.

In the mesh, once x,y,z coordinates are determined, different faces are computed, as some rectangular panels, which have 4 vertexes.

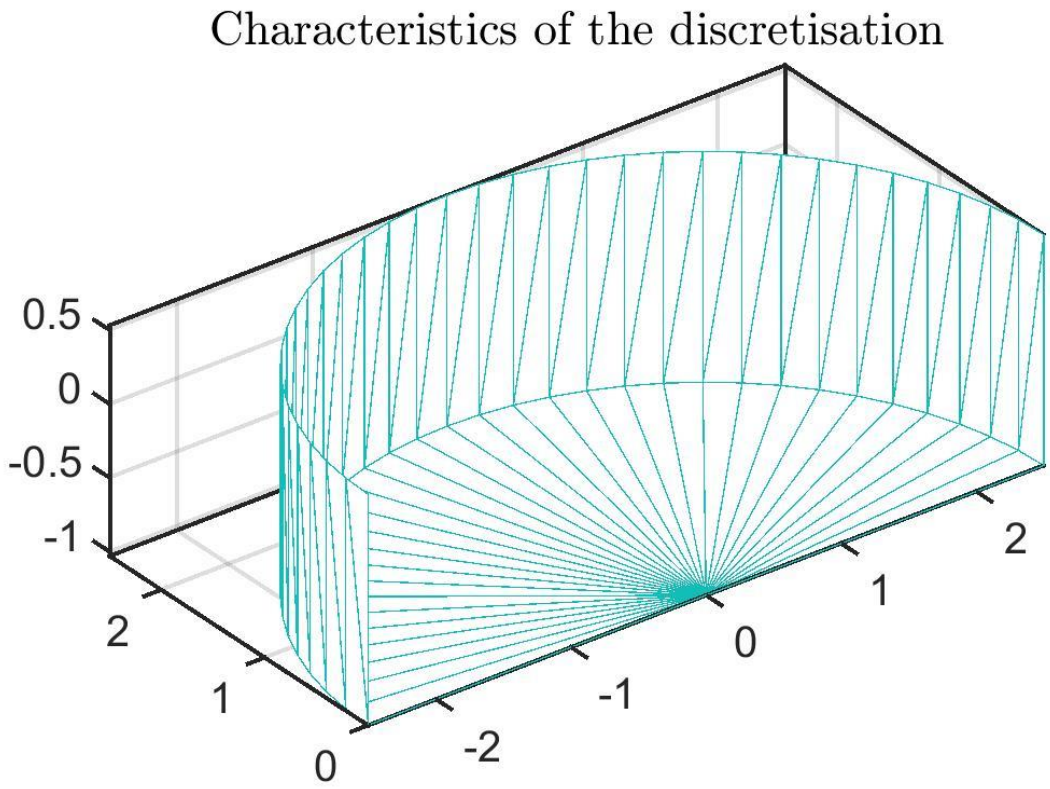

Figure 10:first mesh for the system

This is the first attempt to discretization. For 35 angles, the profile revolution is defined.
With Mesh.exe, these characteristics are discretized, with number of panels already defined, equal to 800.

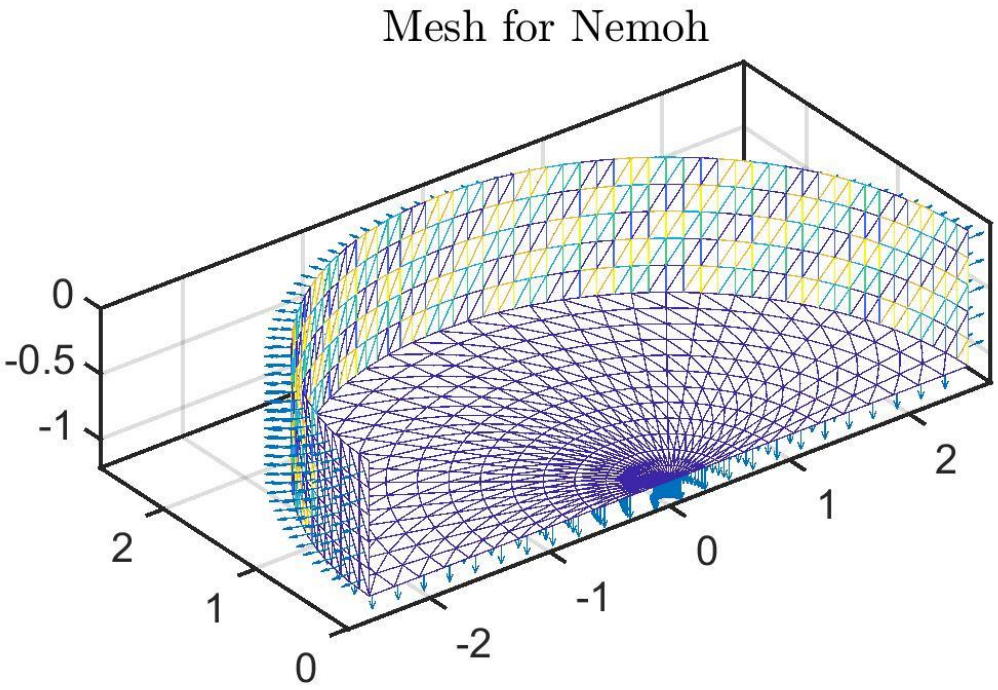

Figure 11: final mesh for the system

From the squared panels, triangular mesh panels are created. This is useful for both visualization and for software itself to operate.
Here, the buoy is cut at z = 0, because it is the wet portion of the buoy. For each panel, there is a vector, which is the normal vector of the panel and goes outwards.
Regarding RAO, it is a transfer function which determines the effect a sea state has on a structure in the water. This is useful in determining the frequencies at which maximum amount of power can be theoretically extracted. It is defined as the ratio between amplitude of motion and amplitude of the wave:

$$RAO(\omega) = \frac{f_k(\omega)}{-\omega^2(m + A(\omega)) + j\omega B(\omega) + K}$$

RAO magnitude and phase are extracted, as function of angular speed ω.

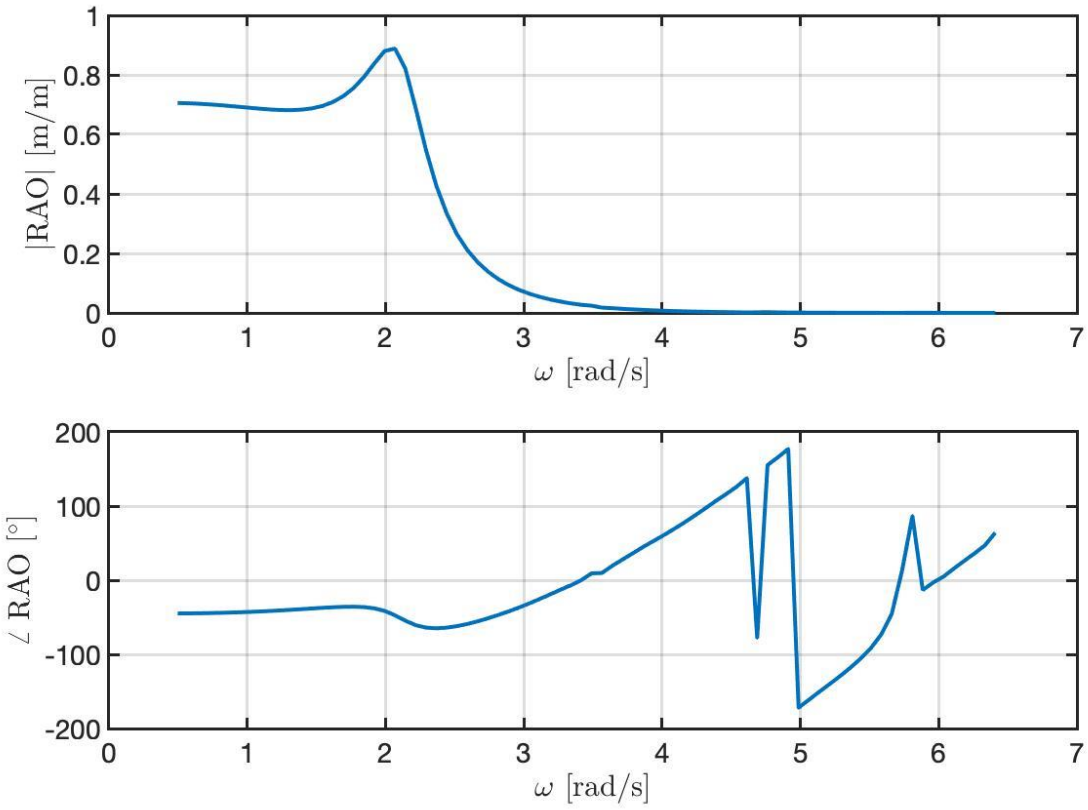

Figure 12: RAO magnitude and phase plots

2.3 Cost function definition

In this part, the productivity has computed. Productivity analysis permits to choose a device among all the examined devices of the parametric run.
A first very gross grid was performed, in which the extreme values are the same of the boundaries of the radius and of the fraction r/h.
In order to perform the study, volume and ballast mass are needed to define. The volume is equal to the volume of a hull cylinder, while, since the buoy is in equilibrium position, the mass of the ballast, is defined as: Archimede's force plus device weight minus external cylinder mass. The material in which the ballast is constructed is concrete.

$$Volume = \pi[r^2 - (r-s)^2] \cdot \frac{r}{h}$$

$$M_{ballast} = Vol_{full} \cdot buoyancy \cdot \rho_{H_2O} - Volume \cdot (1 - buoyancy) \cdot \rho_{mat}$$

where:

- Vol_{full} is the volume of full cylinder: $\pi*r^2*h$.
- Buoyancy is equal to 0.66.
- ρ_{H2O} is the water density, equal to 1025 kg/m^3.
- ρ_{mat} is the considered material density, that are aluminum and fiberglass.

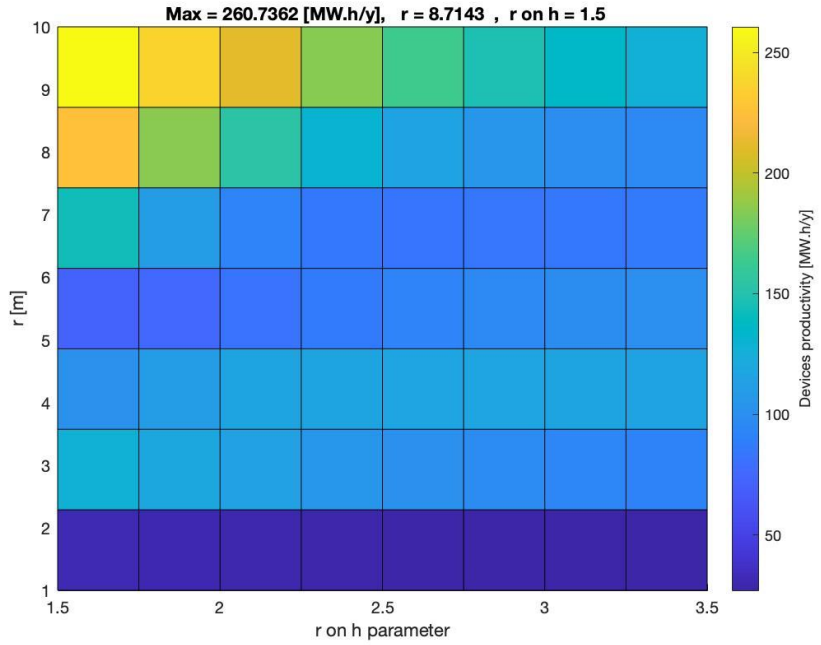

Figure 13: Parametric productivity as function of cylindrical parameters

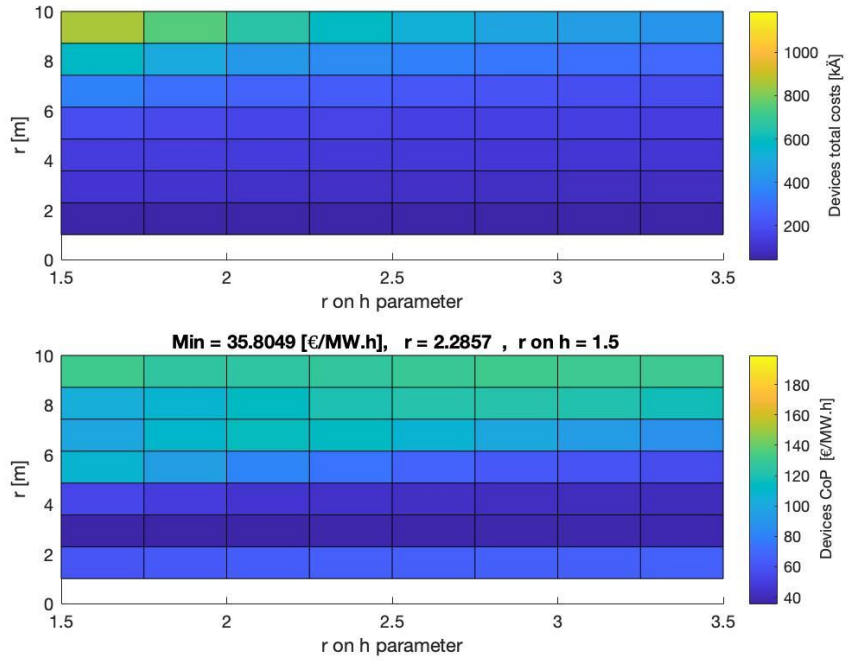

Figure 14: Devices cost and CoP as function of cylindrical parameters

Through these matrices, it is possible to denote what are the values of r and r/h in which the maximum value of productivity and the minimum value of CoP are performed. CoP is the Capex over Productivity, defined as:

$$CoP = \frac{Capex}{N_y AEP}$$

where Ny is the design life, imposed equal to 25 years, while AEP is the annual energy production.
Capex cost, in a simplified model, is equal to:

$$Capex = Device\ cost + mooring\ cost + PTO\ cost$$

How device cost, mooring cost, PTO cost and electrical cable cost are defined, is summarized in the following table:

Device cost	Mooring cost	PTO cost	Electrical cable cost
• Hull cost, calculated with material cost function. • Ballast cost, calculated with concrete cost function.	• A fixed cost due to bathimetry. • A variable cost due to device mass.	• Proportional to device power extraction.	• A fixed cost due to distance from shore.

Table 1: CAPEX costs

For a deeper analysis, device productivity and CoP, function of device cost, are analyzed.

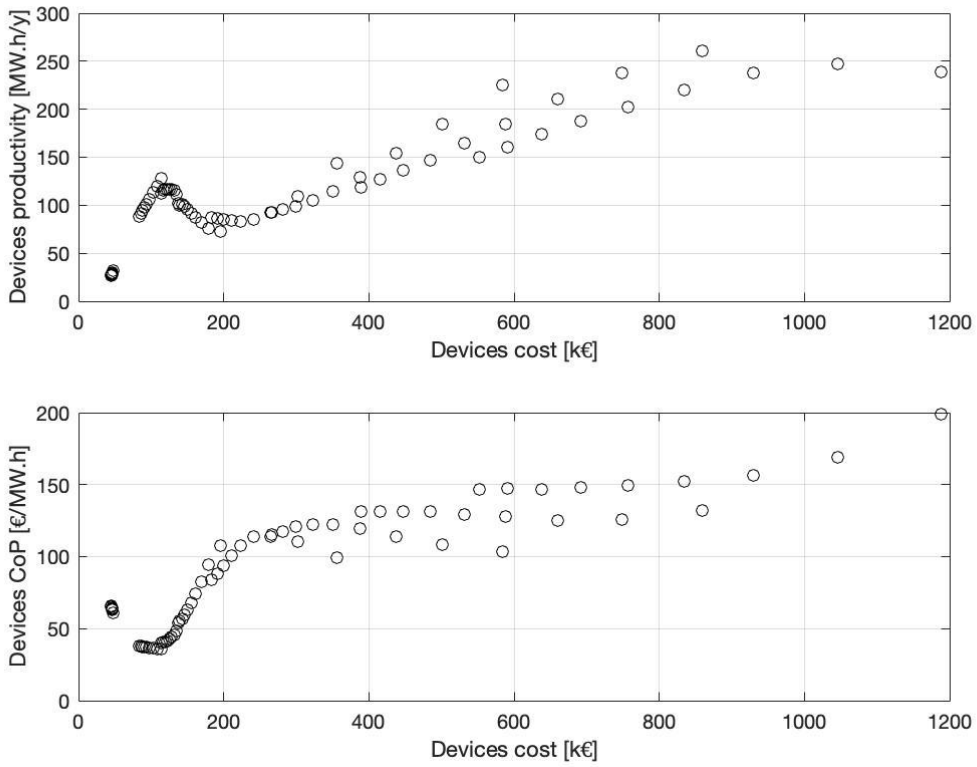

Figure 15: plots of productivity and CoP with respect to the device cost

It is clear that when the productivity presents a maximum, the CoP assumes its minimum value, since they are inversely proportional. Around this point, a more accurate analysis, has been carried out. So, a second grid is performed, in which the best device is probably contained.

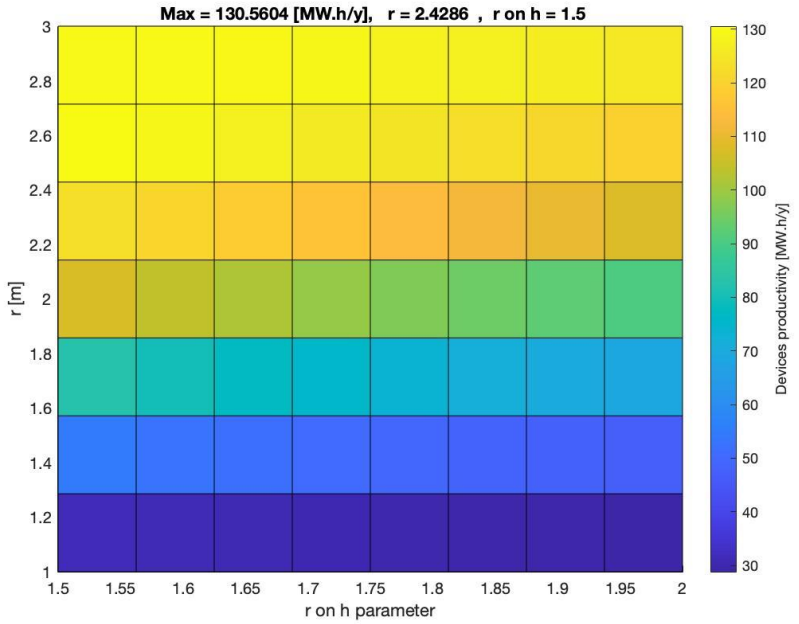

Figure 16: Parametric productivity with a more refined grid

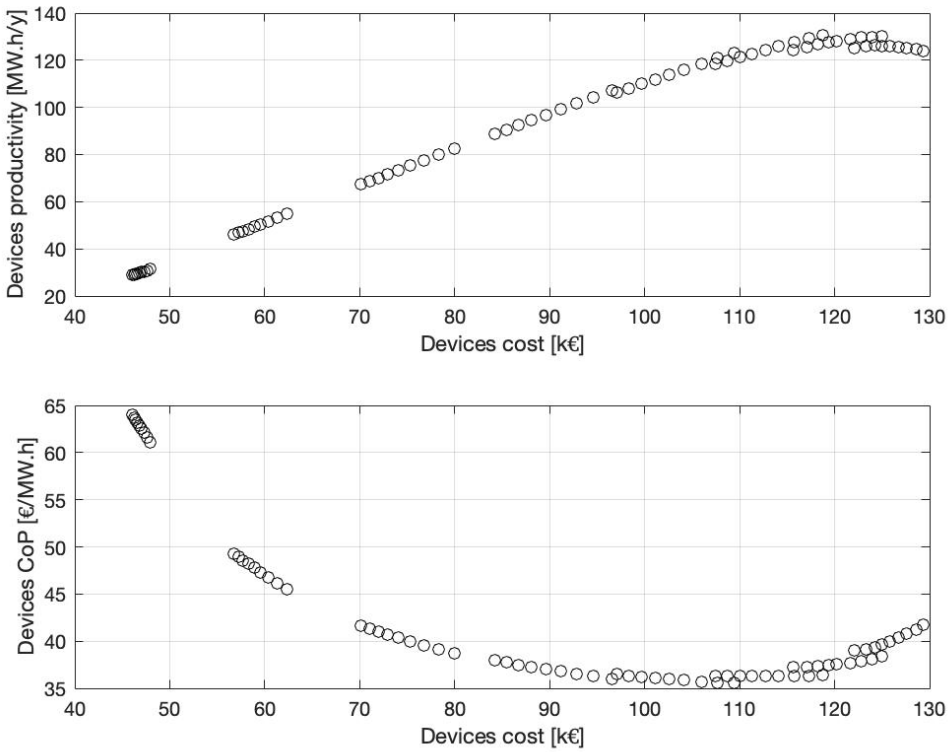

Figure 17: Productivity and CoP of the more refined grid

2.4 Results – device choice

The best device is obtained when r = 2.4286 m, and r/h = 1.5. However, the choice falls into a device with the values:

$$r = 2.5\ m$$
$$\frac{r}{h} = 1.6 \Rightarrow h = 1.5625\ m$$

In this way, there is an easier way to construct the device, since they can be common measures in the applications. Moreover, they are not so distant from the best combination, which presents the maximum productivity and the minimum value of CoP.
With this choice, Nemoh is again launched. This time, a parametric analysis was not performed, because r and r/h were fixed, and all degrees of freedom were computed. Taking the results of the BEM software, Capex of the chosen device was calculated, made of aluminum and fiberglass respectively:

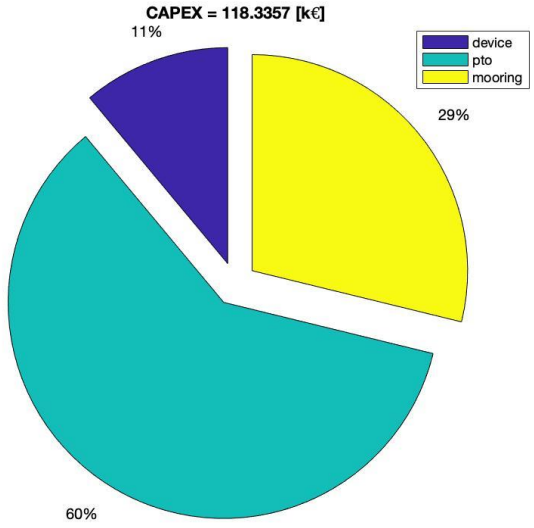

Figure 19: CAPEX of WEC, based on aluminum

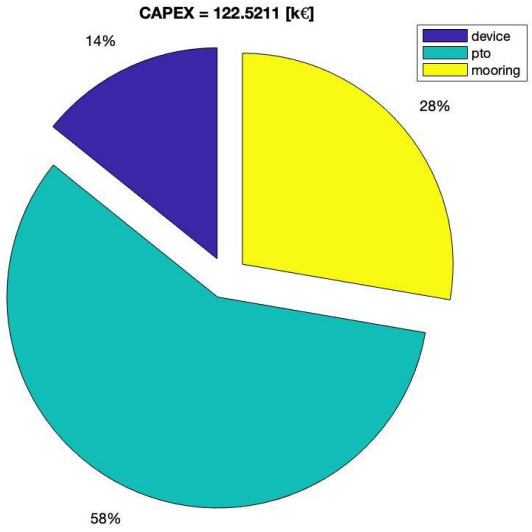

Figure 18: CAPEX of WEC, based on fiberglass

Aluminium	Price [€]	Fraction	**Fiberglass**	Price [€]	Fraction
Device cost [€]	13016,927	11%	Device cost [€]	17152,954	14%
PTO cost [€]	71001,42	60%	PTO cost [€]	71062,238	58%
Mooring cost [€]	34317,353	29%	Mooring cost [€]	34305,908	28%
CAPEX [€]	118335,7	100%	CAPEX [€]	122521,1	100%

Table 2: Detailed CAPEX of both devices

The needed mass of ballast, exclusively made of concrete, is equal to:

- For aluminum case: 2.0145e+04 kg.
- For fiberglass case: 2.0476e+04 kg.

To conclude, cable cost has to be considered, in order to construct a wave farm, which is an installation of multiple WECs. Main goal of this array is to increase the power ratings of installation without increasing the device size, and to reduce LCOE. However, electrical cable is very expensive compared to devices capex. For an electrical cable cost equal to 350,000 €/km, it is required to consider a lot of WECs in order to reduce the cable cost to 35% of a single device Capex.
The distance that was considered is equal to 1.0879 km, so that the electrical cable cost is equal to 380,765 €. To fulfill the request, in both material cases, the minimum number of WECs is equal to 6.

3. Time domain simulations

After the frequency domain simulation, a time domain simulation has been carried out to analyze the behavior of the device using a different model. The simulation has been carried out both with regular and irregular waves. The first was used to find the differences with the frequency analysis of the system, to check the results. The second was used to study the device in a more realistic sea state, such as the irregular one, and to find if the assumptions made in the linear situations still hold. To do that the WEC-SIM code [6] was used on Matlab-Simulink.
In this simulation a time period of 3600 s was considered for the irregular sea state, while in regular sea only 150 s were considered, with 20 s of ramp from no wave to steady state.

3.1 WEC-SIM simulations

To properly use the code, the input data were taken from the results of the frequency analysis. In particular, the best characteristics for the productivity (lowest cost of performance while corresponding to high productivity) were used to choose the best size for the device.
In our specific case the radius for the device was 2.5 m and the ratio r/h was 1.6.
With that some case studies were carried out to have a good picture of the system. In all cases the device moves only in heave, to limit the non-linearities and make easier the interpretation of the results.

1. Case 1: regular waves, optimal damping study. In this case the damping was set equal to the one used for the frequency analysis according to this equation:
   $c_{opt} = \sqrt{B_w^2 + \frac{1}{ww^2} * (-(M + A_w) * ww^2 + Kh)^2}$, where ww is the frequency, M is the total mass of the device, Aw is the coefficient of the hydrodynamic properties, Bw comes from the damping matrix of the simulation with 6 degrees of freedom, and Kh from the hydrodynamic coefficients. To verify this is the best value, a multi condition run (WecSimMCR) was done to calculate the extracted power.

2. Case 2: irregular waves with JONSWAP spectrum, starting from output parameters of the frequency domain analysis. Optimal damping. A fist test was carried out to understand the properties of this wave, so spectrum, height and behavior of the body. Here the values for T_e and H_{m0} were evaluated from the calculation of the Response Amplitude Operator (RAO).

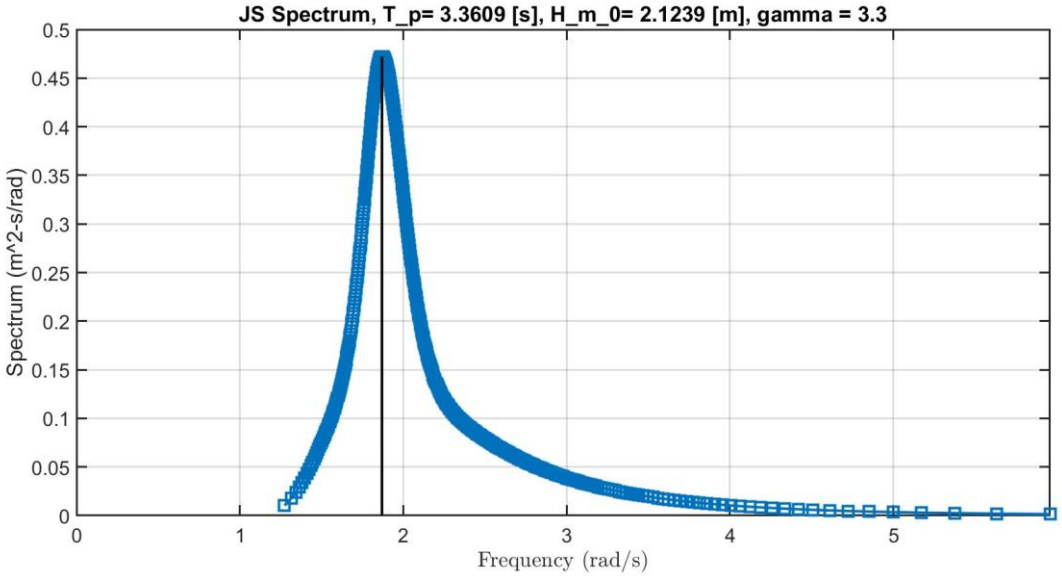

Figure 20: JONSWAP wave spectrum

3. Case 3: irregular waves with JONSWAP spectrum, starting from output parameters of the frequency domain analysis. Variable damping. This test is done to understand if the assumptions made for the frequency analysis still hold for irregular waves. Here the test is done with a simulation time of 3600 s, with a ramp time of around 480 s. Here a range of values from 50% to 100% of the theoretical value have been considered.

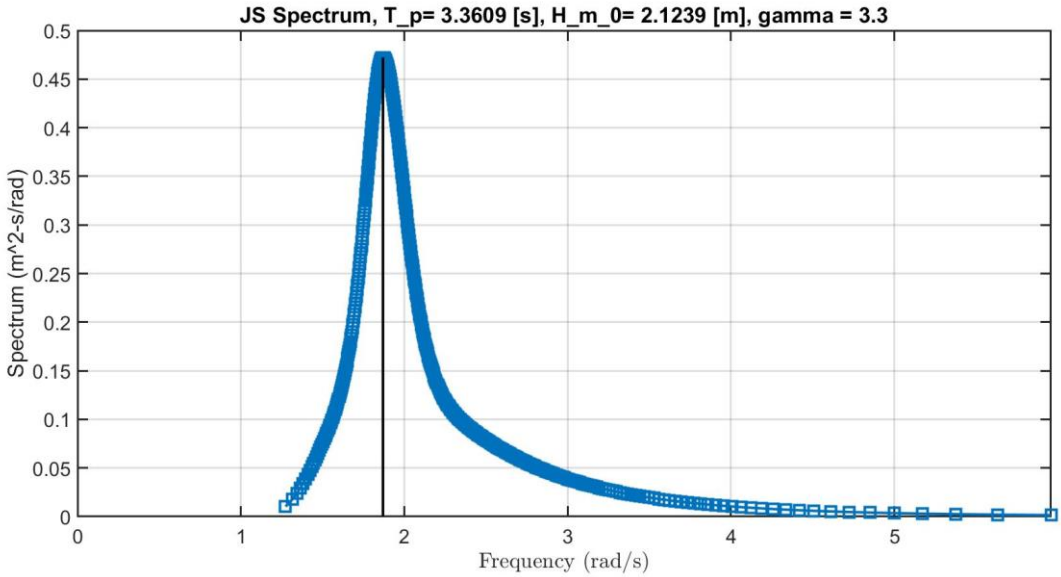

Figure 21: JONSWAP wave spectrum-multi conditions run (MCR)

After a first test with a narrow range of values, which did not show us a law between power and damping, a second one was tested to come out with a trend.

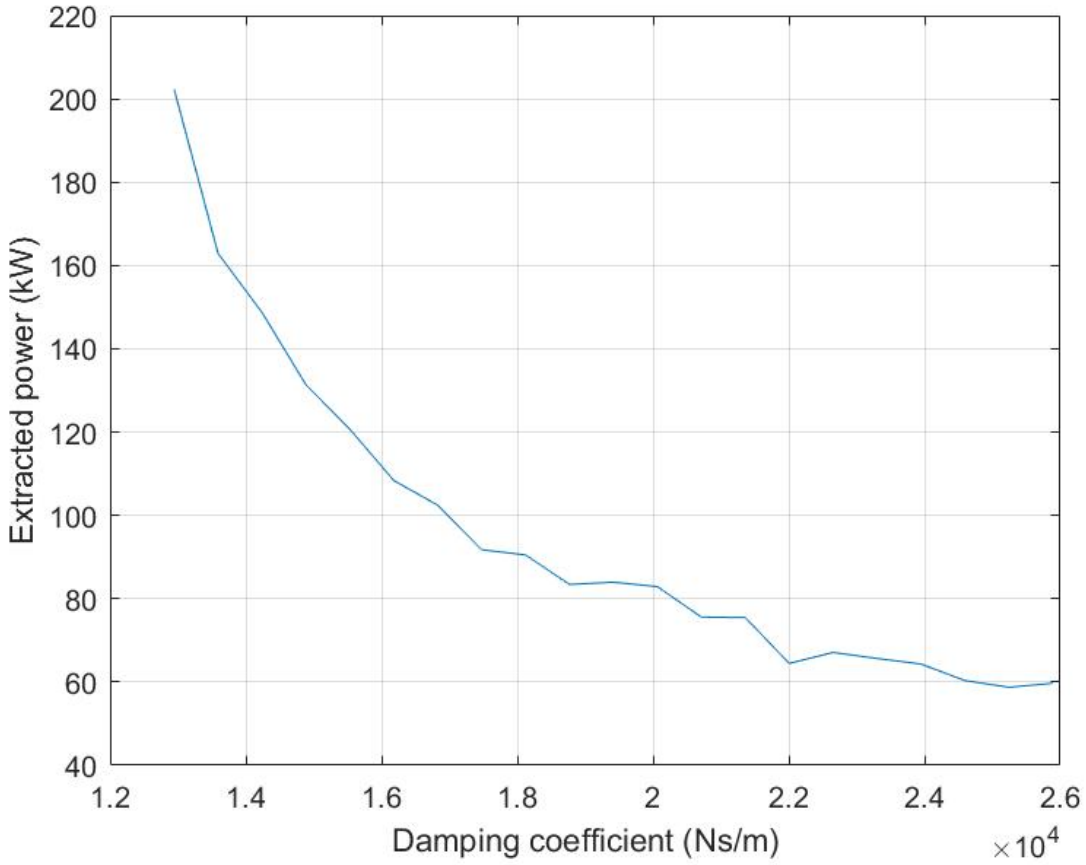

Figure 22:Extracted power with respect to damping coefficient-JONSWAP

3.2 Analysis of the differences between time domain and frequency domain models

Time domain simulation showed us similar results to the frequency analysis mostly under the hypothesis of regular sea state. It was shown from the fact that the coefficients extracted from the NEMOH code were useful also in this case of time model. From the graph, we can see that in regular sea state the damping assumption holds, because in absolute value the maximum extracted power is still located very near to the theoretical optimum (c_{opt}=1.6*10^4 Ns/m).

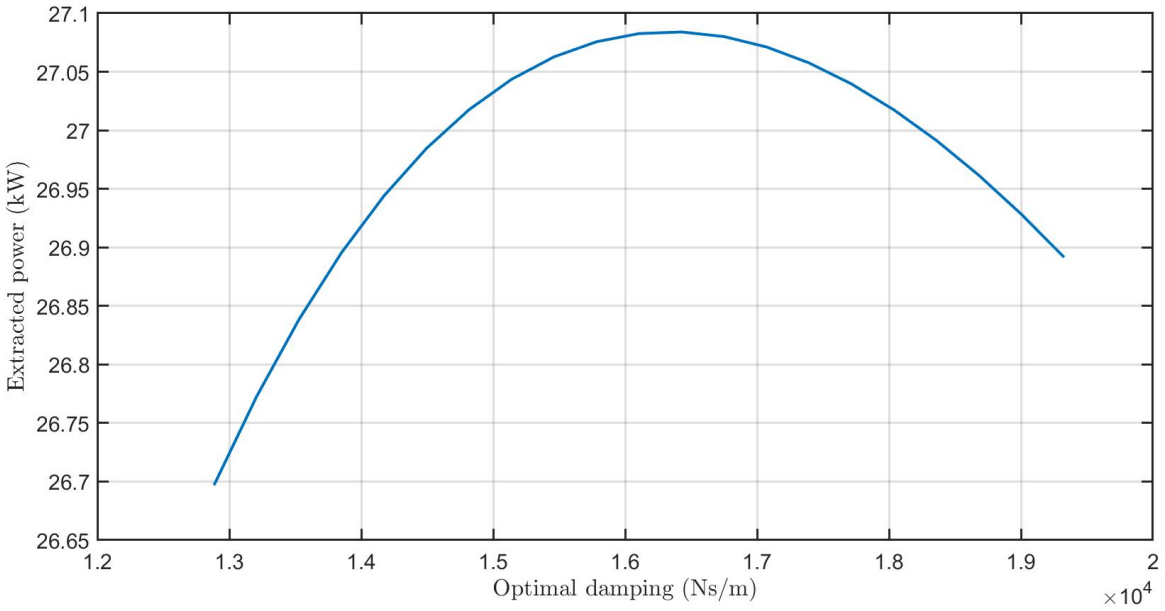

Figure 23: extracted power with respect to damping coefficient (80% to 120% of optimal)-Regular waves

In the case with irregular sea state, instead, these hypotheses are not any more valid. Both the theoretical value changes (it becomes higher, around 2.6*10^4 Ns/m) and there is not any more an optimal power extraction in that point. Here the assumption is no more valid because there is no optimal value for the damping to have maximum power extraction, but only crescent power extractions with decreasing coefficient. The graph below shows the situation for a case with values from 80% to 120% of the theoretical one.

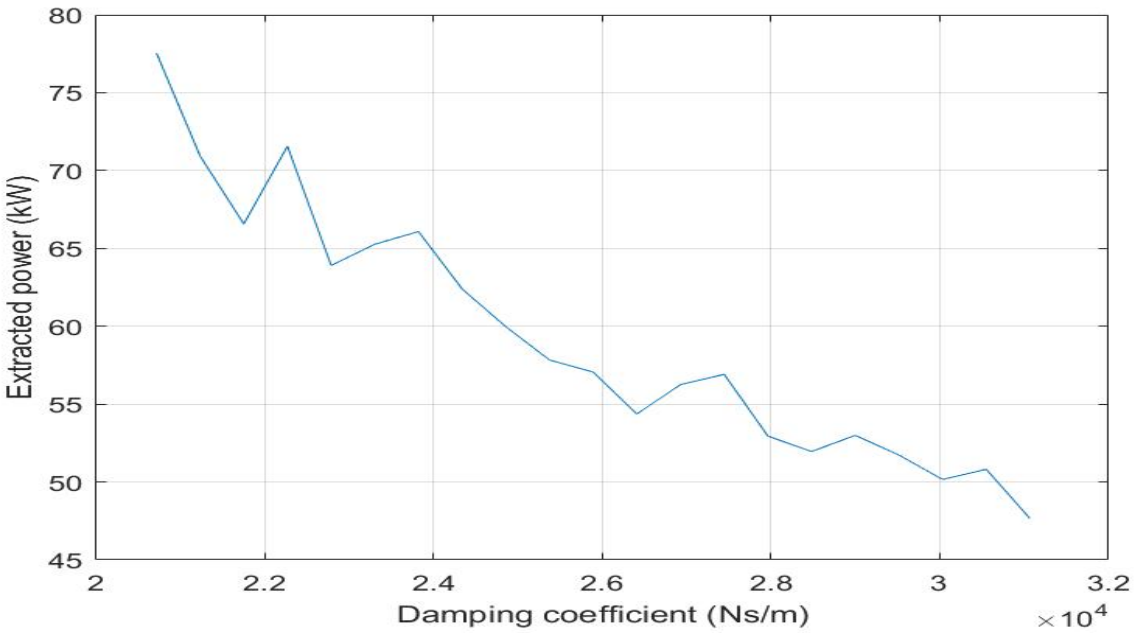

Figure 24:extracted power with respect to damping coefficient (80% to 120% of theoretical value)-JONSWAP

From the figure, it is also possible to notice that the extracted power in irregular sea state is always higher than the case with regular waves. This happens because in this case, that is more realistic, many nonlinear effects are taken into account that were not present in the frequency domain analysis and make no more valid some assumptions valid in the frequency domain analysis.

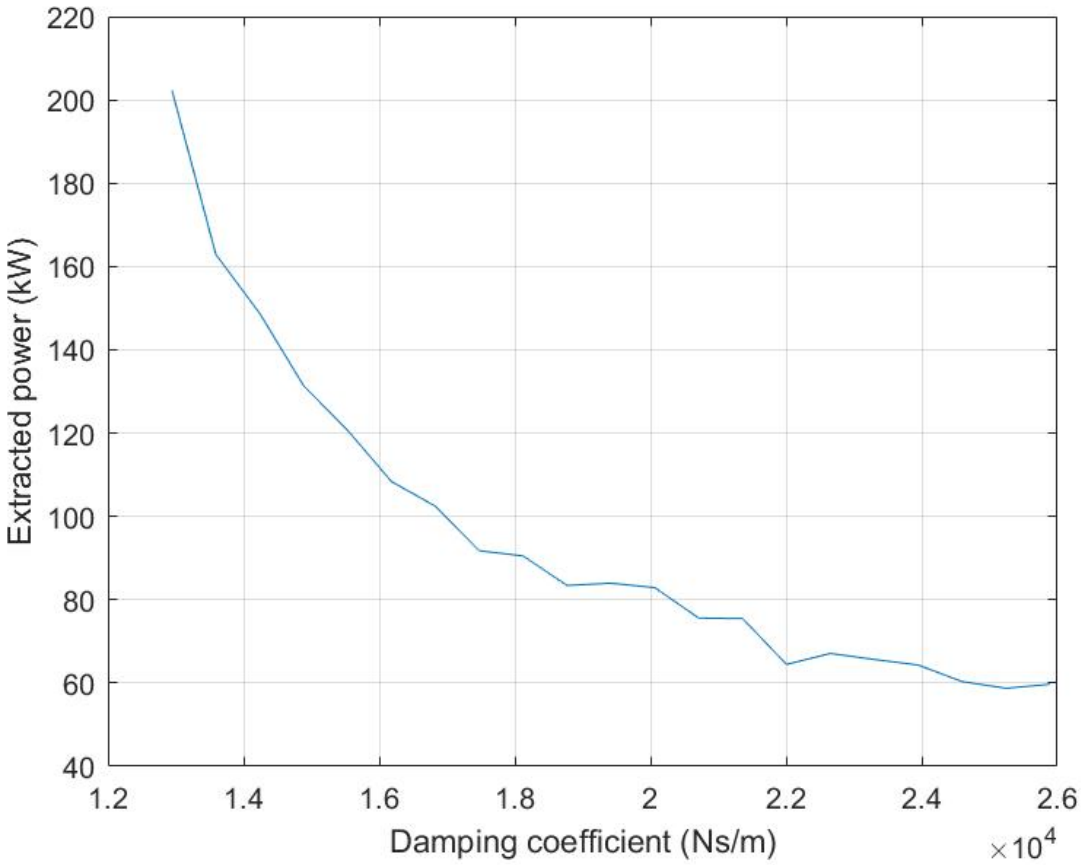

Figure 25: extracted power with respect to damping coefficient (50% to 100% of theoretical value)-JONSWAP

Doing the test with a Multi Condition Run, using a broader range for the damping coefficient (from 50% to 100% of the theoretical value), it is possible to notice that in irregular sea state the power extraction shows an asymptote when the damping goes to values lower than half of the nominal one. It happens probably because if the damping is too low the device can go in resonance, giving a mathematical error in the simulation.

4. Conclusions

In this report, we tried to assess the performances of a point absorber located in Pantelleria island, near Sicilian cost.
From the data provided from ERA5 (mean wave period, mean wave direction, significant combined height), the wave resource assessment has been conducted over the four years of interest (1982, 1986, 1994, 2012) resulting in a wave energy profile adequate (but not excellent) to satisfy the demand of a possible production site.
From the frequency domain analysis, thorough a boundary element method study, the geometrical parametric analysis has been conducted, obtaining the possible combination of COP and productivity as a function of the geometrical parameters of the cylindric point absorber. From this, an optimal device for the condition has been chosen (to have be best possible productivity to cost ratio). This device has then been used as a reference to realize a wave farm of 6 devices (number chosen to match the requested price ratio with the cable cost) capable of exploiting the energy available in that site.
From the time domain analysis, we verified the real, irregular wave performances of the device. This analysis gave out the real parameters of damping and energy production, that are higher lowered with respect to the ideal case in frequency domain. In fact, in real conditions the optimal damping factor tends to zero for this system, this is indicative of the wide real wave spectrum that this system has to endure, hence making it impossible to have an optimal real damping factor. The increased power output is probably due to that in irregular sea state some resonance effects can occur from nonlinearities or from the wave spectrum. They greatly increase the power output in some frequency levels driving up the average power output.

References

1. ERA5,https://cds.climate.copernicus.eu/cdsapp#!/dataset/reanalysis-era5-single-levels?tab=form
2. GOOGLE LCC, «Google Earth,» [Online]. Available: https://www.google.it/intl/it/earth/.
3. Gebco (bathimetry site), https://download.gebco.net/
4. Bret Bosma, Zhe Zhang, Ted K. A. Brekken, H. Tuba Ozkan-Haller, Cameron McNatt, Solomon C. Yim – "Wave Energy Converter Modeling in the Frequency Domain: A Design Guide" – College of Engineering, Oregon State University, Corvallis, USA, 2012
5. Matt Folley – "Numerical Modelling of Wave Energy Converters" – Chapter 2 – 2016
6. http://wec-sim.github.io/WEC-Sim/man/getting_started.html
7. Slides provided by professor G. Bracco